J. Am. Soc. Mass Spectrom. (2016) 27:1277–1284
DOI: 10.1007/s13361-016-1392-2

RESEARCH ARTICLE

Studying Gas-Phase Interconversion of Tautomers Using Differential Mobility Spectrometry

J. Larry Campbell,[1,2] Amy Meng-Ci Yang,[2] Luke R. Melo,[2] W. Scott Hopkins[2]

[1]SCIEX, 71 Four Valley Drive, Concord, ON, Canada L4K 4V8
[2]Department of Chemistry, University of Waterloo, 200 University Ave. West, Waterloo, ON, Canada N2L 3G1

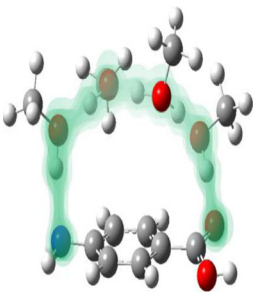

Abstract. In this study, we report on the use of differential mobility spectrometry (DMS) as a tool for studying tautomeric species, allowing a more in-depth interrogation of these elusive isomers using ion/molecule reactions and tandem mass spectrometry. As an example, we revisit a case study in which gas-phase hydrogen-deuterium exchange (HDX)—a probe of ion structure in mass spectrometry—actually altered analyte ion structure by tautomerization. For the N- and O-protonated tautomers of 4-aminobenzoic acid, when separated using DMS and subjected to subsequent HDX with trace levels of D_2O, the anticipated difference between the exchange rates of the two tautomers is observed. However, when using higher levels of D_2O or a more basic reagent, equivalent and almost complete exchange of all labile protons is observed. This second observation is a result of the interconversion of the N-protonated tautomer to the O-protonated form during HDX. We can monitor this transformation experimentally, with support from detailed molecular dynamics and electronic structure calculations. In fact, calculations suggest the onset of bulk solution phase properties for 4-aminobenzoic acid upon solvation with eight CH_3OH molecules. These findings also underscore the need for choosing HDX reagents and conditions judiciously when separating interconvertible isomers using DMS.

Keywords: Microsolvation, Cluster, Tautomerization, Proton-transfer, Gas-phase HDX

Received: 22 January 2016/Revised: 8 March 2016/Accepted: 17 March 2016/Published Online: 19 April 2016

Introduction

The analysis of tautomers—isomeric species that differ only in the positioning of a labile proton [1] —has challenged mass spectrometry (MS) for many decades [2, 3]. In rare cases, orthogonal separation of tautomers prior to MS analysis could be afforded by gas chromatography [4], but the vast majority of cases involve MS analysis of convolved mixtures of tautomers. As such, the probing of tautomeric systems with MS has consisted of observing the relative ratios of tautomers and their fragment ions by adjusting ionization conditions [5], adjusting the energy of a tandem mass spectrometry (MS/MS) event [6], using diagnostic ion/molecule reactions [7–12], probing with ion spectroscopy [13, 14], or through the assistance of computational modeling to confirm the presence and behavior of a given tautomer [15].

More recently, various forms of ion mobility have separated tautomers prior to subsequent MS analysis [16–19]. Among these examples, we described the use of differential mobility spectrometry (DMS) [20–24] to separate the tautomers of protonated 4-ABA (N- and O-protonated) [25]. The primary confirmation for this separation came from the observed tautomers' behavior in the DMS cell and differences in their respective MS/MS fragmentation patterns. However, some questions remained after our use of gas-phase hydrogen-deuterium exchange (HDX) experiments, all implemented by adding HDX reagents in the DMS unit between the DMS cell and the MS orifice. When only using a trace amount of deuterium oxide (D_2O) in the throttle gas, differences in the number of hydrogens exchanged were observed for each 4-ABA tautomer. However, when the amount of D_2O was increased or a more basic HDX reagent was employed (e.g., d_1-methanol, CH_3OD), both tautomers exhibited equivalent numbers of exchanged hydrogens, which we initially interpreted as overexposure of HDX reagent to these ions. However, another

Electronic supplementary material The online version of this article (doi:10.1007/s13361-016-1392-2) contains supplementary material, which is available to authorized users.

Correspondence to: J. L. Campbell; *e-mail:* larry.campbell@sciex.com, W. S. Hopkins; *e-mail*: scott.hopkins@uwaterloo.ca

explanation for this equivalent HDX behavior is that both ions share the same structure as a result of tautomerization during the HDX reaction, converting the N- to the O-protonated form of 4-ABA. Should this be the case, this might also indicate that in DMS experiments, wherein much higher levels of chemical modifiers are used (i.e., ≥1.5% v/v) to enhance ion separation via dynamic clustering, tautomerization could occur in the main section of the DMS cell.

As a tool for structural elucidation, gas-phase HDX has been employed to investigate peptides and proteins [26–28], as well as small molecules [29, 30], and has been implemented in vacuum [31–33], or within atmospheric pressure ion source regions [34]. Depending upon that environment, the mechanism of gas-phase HDX [35, 36] should also be considered. In addition, while HDX generally probes static non-interconvertible structures [37–39], it can also serve to catalyze interconversion (tautomerization) [7–12], thereby complicating the characterization of subtle structural features by MS. However, in the gas-phase HDX studies cited here, the only mechanism for tautomer identification was by observation of changes in ion reactivity within convolved populations; no mechanism for separation of these tautomers before or after identification was available.

Here, we report a more complete characterization of DMS as a tool for separating and characterizing tautomeric populations, along with a detailed investigation of the HDX process within a DMS device for these 4-ABA•H^+ tautomers. Using reactions with D_2O, CH_3OD, and their un-enriched analogues (i.e., H_2O, CH_3OH), we detail how DMS can identify when tautomerization occurs during gas-phase HDX. Although other forms of ion mobility have been employed to separate tautomers [16–19], DMS has some unique advantages for probing such elusive species. For example, DMS has the ability to separate ions based upon subtle differences in their interactions with solvent molecules [22, 24, 40] (and not collision cross section alone); in addition, the relative ease of modifying experimental configurations with rapid change-over of diagnostic ion/molecule reactions (e.g., switch from D_2O to H_2O, etc.), make the analyses of protonated 4-ABA and other DMS-separable tautomers [40] a promising methodology.

Experimental

Materials

4-Aminobenzoic acid, deuterated water, and deuterated methanol were obtained from Sigma-Aldrich (St. Louis, MO, USA) and were used without further purification. HPLC-grade acetonitrile (Caledon Laboratory Chemicals, Georgetown, ON, Canada) and HPLC-grade methanol (J. T. Baker, Avantor Performance Chemicals, Center Valley, PA, USA) were also used without further purification. Distilled deionized water (18 MΩ) was produced in-house using a Millipore Integral 10 water purification system (Billerica, MA, USA).

Differential Mobility Spectrometry/Mass Spectrometry (DMS-MS)

All experiments were conducted using a research-grade DMS [22, 24] system coupled to a hybrid quadrupole linear ion trap mass spectrometer (Figure 1). Briefly, we prepared a 10-ng/mL solution of 4-ABA in 50/50 or 75/25 acetonitrile/water for ESI; these solvent ratios ensured that ESI would generate abundant populations of both N- and O-protonated 4-ABA [25]. To separate the two 4-ABA tautomers, we set the separation voltage (SV) at 3500 V and scanned the compensation voltage (CV) from −15 V to +15 V in 0.1 V increments. At each CV value, we recorded an MS or MS/MS spectrum of 4-ABA•H^+. Each MS and MS/MS experiment for the two tautomers was conducted under identical instrumental conditions. Fragment and residual precursor ions were mass analyzed over the range of *m/z* 50–145 [41].

We implemented gas-phase HDX experiments by adding volatile reagents into the junction chamber between the end of the DMS cell and the orifice of the mass spectrometer. The throttle gas line, normally carrying only nitrogen at 0.2 LPM, was passed through a 500-mL container (VWR) containing either D_2O, H_2O (vapor pressure at 25 °C = 3.169 kPa) [42], CH_3OH, or CH_3OD (vapor pressure at 25 °C = 14.4 kPa). This gas flow that sampled the HDX reagent bottle headspace established a constant number density/pressure of molecules for each tautomer to interact between the terminus of the DMS cell and the sampling orifice of the MS. Some HDX may have taken place after the ions and HDX reagent molecules were sampled by the first vacuum stage of the MS (past the orifice), but the majority of exchange reactions are likely to have occurred within the atmospheric pressure regime of the post-DMS cell region. Although not explicitly measured, the number density of individual HDX reagents and the HDX reaction times were the same for each of the protonated 4-ABA tautomers, given their identical *m/z* values and the equivalent experimental parameters to which both ion populations were subjected. In addition, the time each ion spent in the throttle region can be considered equivalent as all ions experience the same linear gas flow velocity over the same physical space of the throttle region.

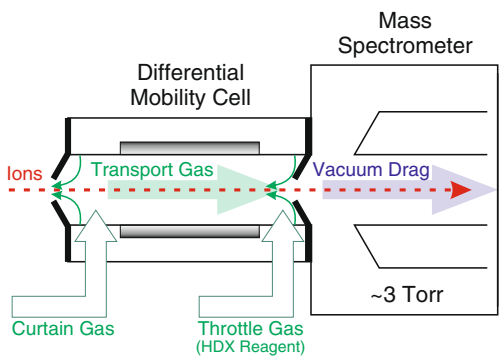

Figure 1. **(a)** Cross-sectional schematic of the differential mobility spectrometer (adapted from Reference [15])

Computational Methods

In support of the experimental work, a detailed computational study of 4-ABA•H^+ microsolvation by CH_3OH was also conducted. First, the basin-hopping (BH) search algorithm was used to identify the low-energy isomers of (4-ABA•H^+)$(CH_3OH)_n$ (n = 1–8) clusters [43–45]. This search employed the AMBER molecular mechanics force field and partial charges for each monomer as calculated at the B3LYP/6-31+G(d,p) level of theory using the CHelpG partition scheme [46–49]. The BH routine sampled degrees of freedom associated with rotation and translation of CH_3OH molecules about a rigid N- or O-protonated 4-ABA core. On each BH iteration, solvent molecules were randomly translated by $-0.7 \le \varphi \le 0.7$ Å in each of the X, Y, and Z directions, and a random rotation of $-5° \le \theta \le 5°$ was applied about each of the solvent body-fixed x, y, and z axes. For clusters containing a single CH_3OH molecule, ~10,000 structures were sampled. This increased to ~30,000 structures for the (4-ABA•H^+)$(CH_3OH)_8$ cluster. Each BH iteration was subject to prescreening with volume and geometry constraints, which ensured that the clusters did not dissociate and that atoms did not occupy the same volume. Convergence criteria for geometry minimization were set to the default values specified by the Gaussian 09 program [50]. BH searches were also supplemented with manually generated chemically intuitive cluster structures.

All unique isomers for the (4-ABA•H^+)$(CH_3OH)_n$ (n = 1–4) clusters that were identified by the BH algorithm were preoptimized at the PM6 and DFTB levels of theory and then input for calculations at the density functional level of theory [51–53]. For the (4-ABA•H^+)$(CH_3OH)_n$ (n = 5–8) species, the 100 lowest energy structures were carried forward for preoptimization and subsequent DFT treatment. DFT calculations were conducted at the B3LYP/6-311++G(d,p) level of theory and normal mode analyses were undertaken for each cluster structure to ensure that it was a local minimum on the potential energy surface. The global minima for the (4-ABA•H^+)$(CH_3OH)_n$ (n = 1–8) series are provided below.

Results and Discussion

We observed previously that the DMS-separated N-protonated and O-protonated 4-ABA each exhibited characteristic behavior in the DMS cell, displayed different HDX patterns, and fragmented differently upon MS/MS [25]. These tautomers were preferentially produced via electrospray ionization (ESI) by judicious selection of the ESI solvents [25, 54, 55]. Earlier confirmation of these two tautomers was achieved by infrared multiple photon dissociation (IRMPD) spectroscopy [55], low-pressure HDX [54], and MS/MS [54, 55]. Figure 2a displays an ionogram of 4-ABA•H^+ recorded at a separation voltage (SV) of 3500 V. Two clearly resolved peaks, the relative populations of which may be controlled by ESI solution conditions, are observed [25, 54, 55]. It is interesting to note the observed shift in peak CV (particularly obvious for the CV = −1.5 V peak) as a function of water concentration. While we do not currently

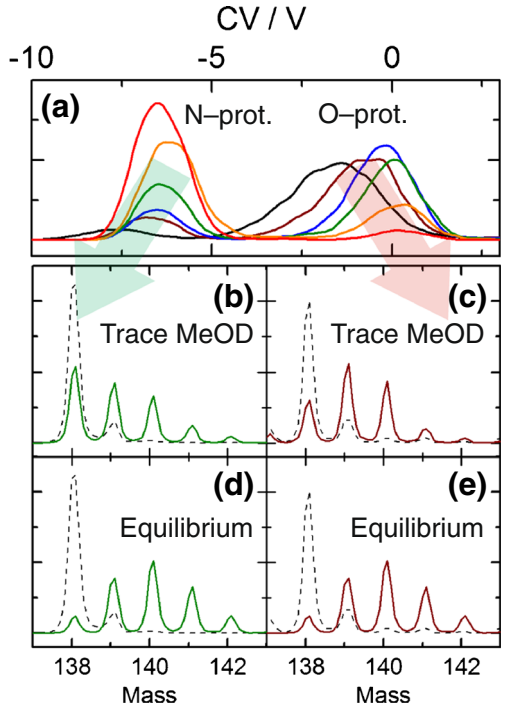

Figure 2. **(a)** Ionogram of the separated tautomers of N- and O-protonated 4-ABA generated under different ESI solvent conditions (acetonitrile/water): red = 100/0; orange = 80/20; green = 60/40; blue = 40/60; purple =20/80; black = 0/100. **(b)** Mass spectrum displaying the isotope pattern for N-protonated 4-ABA (CV = −7.5 V) before (dashed line) and moments after (solid green line) introduction of CH_3OD to the throttle region. **(c)** Mass spectrum displaying the isotope pattern for O-protonated 4-ABA (CV = −1.5 V) before (dashed line) and moments after (solid red line) introduction of CH_3OD to the throttle region. **(d)** Same mass spectrum and CV as **(b)** after CH_3OD has equilibrated. **(e)** Same mass spectrum and CV as **(c)** after CH_3OD has equilibrated

have a definitive explanation for this behavior, it is likely that this phenomenon arises from long-lived ion/water clusters post-ESI. Although these clusters are not observed after ion sampling by the mass spectrometer, we can infer their presence by the more negative (i.e., heavily clustered) 4-ABA•H^+ traces in the ionograms at 100% H_2O compared with the higher percent acetonitrile ESI solution compositions. Several other studies have detailed the strong clustering observed with 100% water solutions in ESI [56–59]. MS/MS of the 4-ABA•H^+ ions isolated at a compensation voltage (CV) of −7.5 V yields (among other product channels) a unique loss of NH_3, whereas isolation and fragmentation of the ions at CV = −1.5 V yields (among others) a more dominant loss of H_2O [25]. These observations are consistent with previous investigations into mixed populations of the 4-ABA•H^+ tautomers [25], and indicate that the peak at CV = −7.5 V is associated with the N-protonated tautomer and that the O-protonated tautomer transmits at CV = −1.5 V.

The DMS-HDX results also support the CV assignments for N- and O-protonated 4-ABA. We observed that the N-protonated 4-ABA•H^+ tautomer, in the presence of a low

partial pressure of D_2O (Supplementary Figure S1B) within the throttle gas (i.e., nitrogen sampled the head space above liquid D_2O in a sealed container), showed slower HDX than the O-protonated tautomer (Supplementary Figure S1C) [25]. This corroborated earlier results [54] where fast HDX was observed for the first two exchanges with the $–COOH_2^+$ group. This difference should be rationalized by considering the differences in gas-phase basicities (GPBs) between the reagent and analyte ions. The degree of HDX should be less for the tautomer with the greatest difference in GPB from that of the HDX reagent [60]. Here, D_2O (GPB_{H2O} = 157.7 kcal/mol) [61] exchanges more hydrogens with O-protonated 4-ABA than N-protonated 4-ABA. While the GPBs of both tautomers (N = 203.2 kcal/mol; O = 207.5 kcal/mol) are greater than H_2O, the ΔGPB for the O- versus N-protonated 4-ABA is −4.3 kcal/mol. Interestingly, the ΔGPB argument is not supported by these and other data that reveal that HDX for O-protonated 4-ABA is faster than for the N-protonated tautomer [25].

However, when D_2O was admitted to the DMS throttle region at a higher number density (i.e., nitrogen was bubbled through the liquid D_2O), all four labile protons associated with the ammonium ($–NH_3^+$) and carboxylic acid (–COOH) groups were exchanged (Supplementary Figure S1D and S1E). As a result, no differentiation between the two tautomers could be made in that HDX experiment. To confirm the critical nature of the gas-phase environment of the DMS, we explored the use of a more basic HDX reagent (i.e., CH_3OD). Interestingly, we noted differences even upon the initial introduction of the reagent at trace levels (Figure 2b and c). These differences quickly disappeared after only a minute's equilibration time (Figure 2d and e). Again, we initially interpreted this result as saturation of the HDX experiment, with all protons exchanged for both tautomers because of the HDX reagent's greater number density (for the D_2O experiment) or because of the more reactive nature of the HDX reagent due to higher GPB (for CH_3OD). However, the possibility of a tautomerization reaction and structural equivalency for both 4-ABA•H^+ isomers could not be discounted.

To explore the possibility of structural transformation induced by the HDX reactions, we probed the 4-ABA•H^+ isomers by MS/MS. By comparing the fragmentation patterns of the two DMS-separated tautomers—with and without HDX reactions—we could discern the impact (if any) HDX reactions have on ion structure. To simplify these experiments and the resulting MS/MS fragmentation patterns, we replaced the HDX reagents with their protonated analogues (e.g., H_2O for D_2O) under the assumption that the ion/molecule reactions (i.e., HDX or proton exchange) would be equivalent (except for the lack of deuteriums). By performing MS/MS on these ions (and not their deuterated analogues), we could assess any telling changes to the tautomers' fragmentation patterns without concern for additional isotope scrambling that occurs during MS/MS.

Without any throttle gas additives (i.e., nitrogen only), the MS/MS of the N-protonated 4-ABA•H^+ (*m/z* 138) ions (CV = −7.5 V) showed expected NH_3 loss and residual precursor ion (characteristic of N-protonated) (Figure 3b), while at CV = −1.5 V, the MS/MS spectra contained very little residual

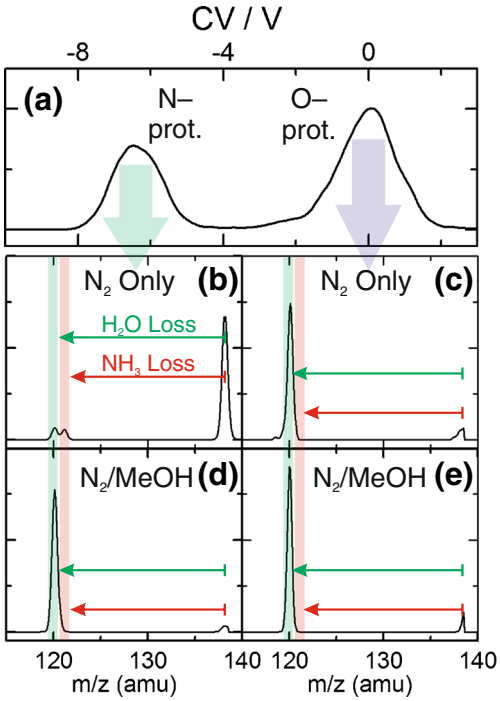

Figure 3. **(a)** Ionogram of the separated tautomers of N- and O-protonated 4-ABA. **(b)** MS/MS spectrum for N-protonated 4-ABA (*m/z* 138; CV = –7.5 V) with only N_2 in the throttle gas. **(c)** MS/MS spectrum for O-protonated 4-ABA (*m/z* 138; CV = –1.5 V) with only N_2 in the throttle gas. **(d)** MS/MS spectrum for N-protonated 4-ABA (*m/z* 138; CV = –7.5 V) with CH_3OH in the throttle gas. **(e)** MS/MS spectrum for O-protonated 4-ABA (*m/z* 138; CV = –1.5 V) with CH_3OH in the throttle gas. All MS/MS spectra were acquired using the same lab-frame collision energy of 30 eV

precursor ion and loss of water as the base peak, indicative of the O-protonated 4-ABA (Figure 3c). However, upon addition of CH_3OH to the throttle region, the MS/MS spectrum for the N-protonated 4-ABA•H^+ changed dramatically (Figure 3d) and was now exactly the same as the O-protonated species at CV = −1.5 V (Figure 3e). The same observations were made when water was added to the throttle gas instead of methanol (Supplementary Figure S4). Therefore, we postulate that, as a result of introducing CH_3OH (or CH_3OD in the HDX experiments), we tautomerized the N-protonated 4-ABA•H^+ to the more energetically stable O-protonated tautomer post DMS separation; similar findings were obtained when H_2O was added to the throttle gas instead of CH_3OH (Supplementary Figure S2). It is worth noting that a minor loss of H_2O is observed following collision induced dissociation (CID) for the N-protonated species, even in experiments that did not introduce a HDX reagent. It is well known that CID (MS/MS) can cause structural scrambling. However, the two MS/MS patterns here are different enough to rationalize the originating tautomers. It is also possible, of course, that a low-partial pressure (i.e., trace amount) of HDX reagent could similarly result in a minor degree of tautomerization in the (nominally) pure N_2 environment.

However, given the relatively minor degree of tautomerization introduced by CID (which is much more agressive in an energetic

sense than HDX) and the relatively short ms-timescale for our HDX experiments, we expect that the extent of tautomerization in a low-pressure environment should be small. Considering these MS/MS experiments, we suggest that the near equivalent HDX behavior of the N- and O-protonated tautomers with CH_3OD was not the result of HDX saturation but was, instead, a tautomerization reaction, with equivalent HDX observed because the actual ionic structures were identical.

Our experimental results are consistent with the data and subsequent hypotheses of earlier researchers in the field of gas-phase HDX [35]. These groups postulated that one of the possible HDX modes follows a "relay mechanism" whereby the HDX reagent exchanges a proton at the site of the analyte molecule's protonation while transferring one of its deuteriums to an atom initially distal to the analyte molecule's original site of protonation. While these studies were conducted at very low pressures where single HDX reagent/analyte ion interactions were presumed dominant, we propose that a similar form of "relay mechanism" is also occurring in the atmospheric pressure HDX reactions considered here, with multiple reagent molecules playing roles.

To understand how ion/solvent clusters in the post-DMS region may be involved in such an HDX "relay mechanism," we performed basin hopping (BH) searches of the potential energy landscape for (4-ABA•H^+)$(CH_3OH)_n$ (n = 1–8) clusters [43–45]. As a result, we identified three different structural motifs: N-protonated, O-protonated, and solvent-bridged. In N-protonated structures, the proton and its charge are localized at the nitrogen center forming an $–NH_3^+$ moiety. For N-protonated clusters containing relatively few solvent molecules (i.e., n ≤ 5), CH_3OH binds to the charged end of the 4-ABA•H^+ (Supplementary Figure S3). As additional CH_3OH molecules are added (i.e., n ≥ 6), clustering also begins to occur about the carboxylic acid end of N-protonated 4-ABA. Similar clustering behavior is observed for the O-protonated structures (Supplementary Figure S4). However, initial clustering (for n ≤ 4) is localized around the protonated carboxylic acid end of the molecule. Only at n ≥ 5 does CH_3OH begin to solvate the $–NH_2$ group of O-protonated 4-ABA•H^+. Typically, these clusters exhibit ion-solvent hydrogen-bonding networks when there are three or more CH_3OH molecules in relatively close proximity (Supplementary Figure S5).

At n ≥ 3, solvent-bridged structural motifs were also calculated for (4-ABA•H^+)$(CH_3OH)_n$ clusters (Supplementary Figure S5). These structures typically exhibit hydrogen-bonded chains of three or four CH_3OH molecules, extending from the amine group to the carbonyl oxygen. The n = 3 and n = 4 solvent-bridged structures of (4-ABA•H^+)$(CH_3OH)_n$ (see Figure 4) reveal that the proton is located within the hydrogen-bond network for both of these clusters. The appearance of bridging hydrogen-bond networks like these suggests that tautomerization in (4-ABA•H^+)$(CH_3OH)_n$ clusters occurs by proton transfer or shuttling along a hydrogen-bond network of methanol molecules via a Grotthuss-like mechanism [62].

Figure 5 plots the zero-point-corrected electronic energies of the lowest energy solvent-bridged and solvated O-

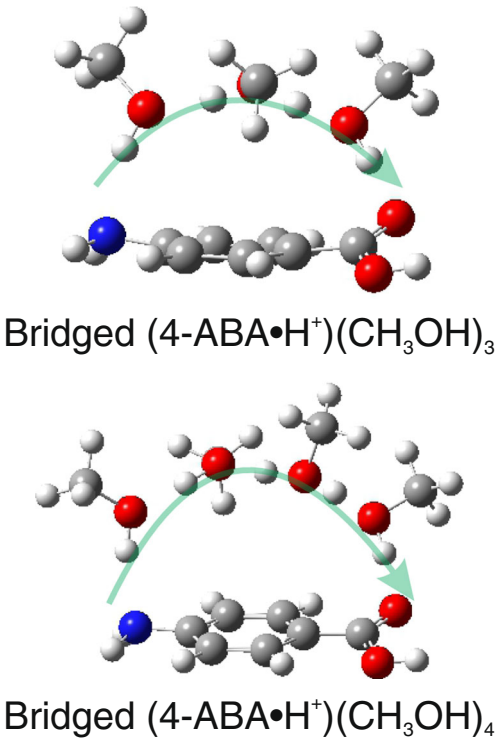

Figure 4. The geometry optimized solvent-bridged structures of (4-ABA•H^+)$(CH_3OH)_n$ (n = 3, 4) [B3LYP-GD3/6-311++G(d,p)]

protonated structures relative to the lowest energy solvated N-protonated structure for each (4-ABA•H^+)$(CH_3OH)_n$ (n = 0–8) cluster. (N.B. These reported energies are D_0 and not Gibbs free energies as the precise temperature of the ions is not well

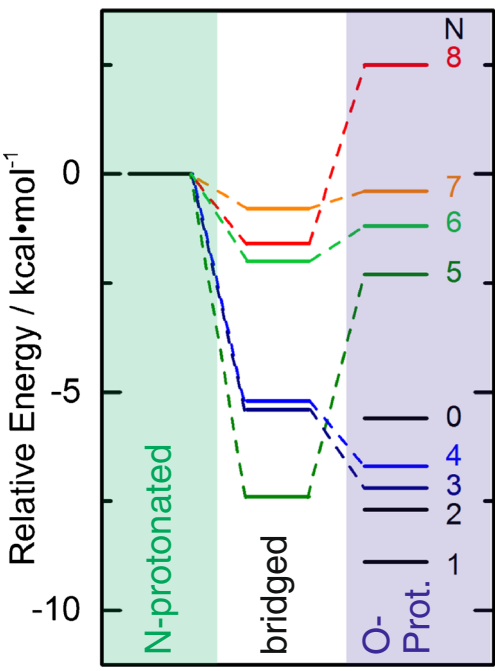

Figure 5. Calculated zero-point-corrected electronic energies of the (center) bridged and (right) O-protonated isomers of (4-ABA•H^+)$(CH_3OH)_n$ (n = 1– 8) relative to the associated N-protonated structures [B3LYP-GD3/6-311++G(d,p)]

characterized due to field-induced heating of the ions in the DMS cell; further studies into this area are presently underway). Interestingly, although the N-protonated form of 4-ABA•H^+ is the most stable tautomer in protic solution [63], the O-protonated structure is most stable when isolated in the gas-phase. Here, we calculate that O-protonated 4-ABA•H^+ is 5.6 kcal•mol^{-1} lower in energy than the N-protonated tautomer, which is in excellent agreement with earlier reported ranges of 4.1–9.5 kcal•mol^{-1} [54, 55]. Interestingly, we find that adding a CH_3OH molecule stabilizes the O-protonated structure relative to the N-protonated form by a further 3.3 kcal•mol^{-1}. However, with the addition of more CH_3OH molecules, the O-protonated tautomer becomes increasingly destabilized until at n = 8 the N-protonated structure becomes thermodynamically favoured. This marks the onset of solution phase properties with respect to basicity. This finding is supported by an earlier IR photodissociation spectroscopy/computational study [64] that demonstrated that when fewer than 6 H_2O molecules were bound to 4-ABA•H^+, the O-protonated tautomer was more stable and abundant. However, with 6 and more H_2O molecules, the N-protonated tautomer (i.e., the more stable tautomer in protic liquid) was more stable and abundant. This interconversion via the proton shuttling efforts of polar molecules (e.g., H_2O, CH_3OH) has also been suggested for many other small ionic isomer systems (e.g., distonic and conventional radical cations) [7–12, 36], although none were separated prior to analysis in the gas-phase as DMS has provided here.

From n = 5 – 8, it is the solvent-bridged structures that are the global minima for (4-ABA•H^+)$(CH_3OH)_n$ clusters. This has important bearing on the observed tautomerization; if the HDX reagent is of sufficient partial pressure to form (4-ABA•H^+)$(CH_3OD)_n$ ($n \geq 5$) when clustering occurs in the atmospheric pressure environment, it will anneal to its lowest-energy structures and sample the solvent-bridged configuration. This will transfer the proton to the solvent-bridge hydrogen bond network. As the cluster then de-solvates during its transit from the ion source (atmospheric pressure) into the mass spectrometer's first vacuum stage (where electrode positioning and voltages serve to desolvate clustered ions) [65], it becomes thermodynamically favorable to deposit the proton onto the carbonyl oxygen. (It is this configuration of electrodes in this mass spectrometer that disrupts most ion/solvent clusters, preventing their direct analysis using the present instrumentation). In the case of the O-protonated tautomer, the proton will remain localized on the carbonyl oxygen if small clusters ($n \leq 4$) are formed, or it will transfer to the solvent-bridge hydrogen bond network and back to the carbonyl oxygen if clusters in the n = 5–7 range are formed. For the N-protonated structure, if only small clusters are produced (i.e., n = 1, 2), the solvent bridge cannot form and the proton remains kinetically trapped on the nitrogen center. Should clusters with n = 3–8 form, the cluster will isomerize to the solvent bridged structure, the proton will be transferred to the solvent bridge hydrogen bond network, and subsequently to the carbonyl oxygen upon desolvation.

Conclusions

In this study, we have demonstrated the utility of DMS as a tool to study tautomeric ions, using the DMS behavior, gas-phase HDX reactions, and MS/MS. In addition, the use of DMS allows for the observation of subtle structural changes via tautomerization when ion/molecule reactions (like HDX) are employed. For N-protonated and O-protonated 4-ABA, we observed that the DMS-separated tautomers lose their distinct HDX and MS/MS characteristics upon addition of moderate-to-high HDX reagent concentrations prior to MS analysis. Detailed and extensive molecular dynamics and electronic structure calculations show that with increased solvation, the O-protonated form of 4-ABA•H^+ is destabilized with respect to the N-protonated structure. This suggests that when clusters reach a critical size, a Grotthuss-type mechanism may concurrently provide HDX functionality while tautomerizing N-protonated 4-ABA to its more stable gas-phase analogue—O-protonated 4-ABA. These findings underscore the fact that care should be taken when performing HDX experiments, especially under atmospheric pressure conditions. In addition, one should be aware of the possibility that subtle structural changes, such as tautomerization, could occur in DMS experiments when employing chemical modifiers to enhance separations. Such changes could be utilized to an advantage (e.g., convert all ion signal into one tautomeric form with one optimal set of DMS conditions) for higher signal-to-noise measurements of the base molecular substructure (e.g., only O-protonated 4-ABA would be detected as "4-ABA" not both tautomers). Overall, the DMS' experimental configuration provides several orthogonal avenues of investigation for tautomeric species, in addition to other interesting isomeric systems.

Acknowledgments

The authors thank Dr. Bradley Schneider and Dr. Yves Le Blanc (SCIEX), as well as Professor Terry McMahon (University of Waterloo), for helpful discussions and feedback. The authors also acknowledge funding from the Natural Sciences and Engineering Research Council (NSERC) of Canada and high performance computing resources from the Sharcnet consortium of Compute Canada.

References

1. Taylor, P.J., van der Zwan, G., Antonov, L.: Tautomerism: introduction, history, a recent developments in experimental and theoretical methods. In: Antonov, L. (ed.) Tautomerism: methods and theories, pp. 1–24. Wiley-VCH Verlag GmbH and Co, Weinheim (2014)
2. Terent'ev, P.B., Kalandarishvili, A.G.: Application of mass spectrometry for the analysis of organic tautomeric compounds. Mass Spectrom. Rev. **15**, 339–363 (1996)
3. Furlong, J.J.P., Schiavoni, M.M., Castro, E.A., Allegretti, P.E.: Mass spectrometry as a tool for studying tautomerism. Rus. J. Org. Chem. **44**, 1725–1736 (2008)
4. Masur, M., Grützmacher, H.-F., Münster, H., Budzikiewicz, H.: Mass spectrometric fragmentation of the tautomers of 1,3-diketones: a gas chromatography/mass spectrometric study. Org. Mass Spectrom. **22**, 493–500 (1987)

5. Zamir, L., Jensen, B.S., Larsen, E.: An investigation of tautomeric equilibria by means of mass spectrometry. Org. Mass Spectrom. **2**, 49–61 (1969)
6. Kenttämaa, H.I., Cooks, R.G.: Tautomer characterization by energy resolved mass spectrometry. Dimethyl phosphite and dimethyl phosphonate ions. J. Am. Chem. Soc. **107**, 1881–1886 (1985)
7. Stewart, J.H., Shapiro, R.H., Depuy, C.H., Bierbaum, V.M.: Hydrogen-deuterium exchange reactions of carbanions with D_2O in gas phase. J. Am. Chem. Soc. **99**, 7650–7653 (1977)
8. Andrist, A.H., DePuy, C.H., Squires, R.R.: Structures of isomeric anions in the gas phase. Arylallyl and arylcycloproyl anions. J. Am. Chem. Soc. **106**, 845–850 (1984)
9. DePuy, C.H., Bierbaum, V.M., Damrauer, R., Soderquist, J.A.: Gas-phase reactions of the acetyl anion. J. Am. Chem. Soc. **107**, 3385–3386 (1985)
10. Polfer, N.C., Dunbar, R.C., Oomens, J.: Observation of Zwitterion formation in the gas-phase H/D-exchange with CH_3OD: solution-phase structures in the gas phase. J. Am. Soc. Mass Spectrom. **18**, 512–516 (2007)
11. Audier, H.E., Leblanc, D., Mourgues, P., McMahon, T.B., Hammerum, S.: Catalyzed isomerization of simple radical cations in the gas-phase. J. Chem. Soc. Chem. Commun. 2329–2330 (1994) http://pubs.rsc.org/en/content/articlelanding/1994/c3/c39940002329#!divAbstract
12. Gauld, J.W., Audier, H., Fossey, J., Radom, L.: Water-catalyzed interconversion of conventional and distonic radical cations: methanol and methyleneoxonium radical cations. J. Am. Chem. Soc. **118**, 6299–6300 (1996)
13. Steill, J.D., Oomens, J.: Gas-phase deprotonation of p-hydroxybenzoic acid investigated by IR spectroscopy: solution-phase structure is retained upon ESI. J. Am. Chem. Soc. **131**, 13570–13571 (2009)
14. Almasian, M., Grzetic, J., van Maurik, J., Steill, J.D., Berden, G., Ingemann, S., Buma, W.J., Oomens, J.: Non-equilibrium isomer distribution of the gas-phase photoactive yellow protein chromophore. J. Phys. Chem. Lett. **3**, 2259–2263 (2012)
15. Wu, R., McMahon, T.B.: Investigation of proton transport tautomerism in clusters of protonated nucleic acid bases (cytosine, uracil, thymine, and adenine) and ammonia by high-pressure mass spectrometry and ab initio calculations. J. Am. Chem. Soc. **129**, 569–580 (2007)
16. Karpas, Z., Berant, Z., Stimac, R.M.: An ion mobility spectrometry/mass spectrometry (IMS/MS) study of the site of protonation in anilines. Struct. Chem. **1**, 201 (1990)
17. Lalli, P.M., Iglesias, B.A., Toma, H.E., de Sa, G.F., Daroda, R.J., Silva Filho, J.C., Szulejko, J.E., Araki, K., Eberlin, M.N.: Protomers: formation, separation, and characterization via traveling wave ion mobility mass spectrometry. J. Mass Spectrom. **47**, 712–719 (2012)
18. Schröder, D., Buděšínský, M., Roithová, J.: Deprotonation of p-hydroxybenzoic acid: does electrospray ionization sample solution- or gas-phase structures? J. Am. Chem. Soc. **134**, 15897–15905 (2012)
19. Warnke, S., Seo, J., Boschmans, J., Sobott, F., Scrivens, J.H., Bleiholder, C., Bowers, M.T., Gewinner, S., Schollkopf, W., Pagel, K., von Helden, G.: Protomers of benzocaine: solvent and permittivity dependence. J. Am. Chem. Soc. **137**, 4236–4242 (2015)
20. Eiceman, G., Karpas, Z.: Ion mobility spectrometry. CRC Press, Boca Raton, FL (2005)
21. Krylov, E.V., Nazarov, E.G., Miller, R.A.: Differential mobility spectrometer: model of operation. Int. J. Mass Spectrom. **266**, 76–85 (2007)
22. Schneider, B.B., Covey, T.R., Coy, S.L., Krylov, E.V., Nazarov, E.G.: Planar differential mobility spectrometer as a pre-filter for atmospheric pressure ionization mass spectrometry. Int. J. Mass Spectrom. **298**, 45–54 (2010)
23. Shvartsburg, A.A.: Differential Ion mobility spectrometry: nonlinear Ion transport and fundamentals of FAIMS. CRC Press, Boca Raton, FL (2009)
24. Campbell, J.L., Zhu, M., Hopkins, W.S.: Ion-molecule clustering in differential mobility spectrometry: lessons learned from tetraalkylammonium cations and their isomers. J. Am. Soc. Mass Spectrom. **25**, 1583–1591 (2014)
25. Campbell, J.L., Le Blanc, J.C.Y., Schneider, B.B.: Probing electrospray ionziation dynamics using differential mobility spectrometry: the curious case of 4-aminobenzoic acid. Anal. Chem. **84**, 7857–7864 (2012)
26. Katta, V., Chait, B.T.: Conformational changes in proteins probed by hydrogen exchange electrospray ionization mass spectrometry. Rapid Commun. Mass Spectrom. **5**, 214–217 (1991)
27. Konermann, L., Pan, J.X., Liu, Y.H.: Hydrogen exchange mass spectrometry for studying protein structure and dynamics. Chem. Soc. Rev. **40**, 1224–1234 (2011)
28. Wales, T.E., Engen, J.R.: Hydrogen exchange mass spectrometry for the analysis of protein dynamics. Mass Spectrom. Rev. **25**, 158–170 (2006)
29. Squires, R.R., DePuy, C.H., Bierbaum, V.M.: Gas-phase hydrogen-deuterium exchange reactions in carbanions. Exchange of vinyl and aryl protons by D_2O. J. Am. Chem. Soc. **103**, 4256–4258 (1981)
30. DePuy, C.H., Bierbaum, V.M., King, G.K., Shapiro, R.H.: Hydrogen-deuterium exchange reactions of carbanions with deuterated alcohols in the gas phase. J. Am. Chem. Soc. **100**, 2921–2922 (1978)
31. Hunt, D.F., McEwen, C.N., Upham, R.A.: Determination of active hydrogen organic compounds by chemical ionization mass spectrometry. Anal. Chem. **44**, 1292–1294 (1972)
32. Freiser, B.S., Woodin, R.L., Beauchamp, J.L.: Sequential deuterium exchange reactions of protonated benzenes with D_2O in gas-phase by ion cyclotron resonance spectroscopy. J. Am. Chem. Soc. **97**, 6893–6894 (1975)
33. Suckau, D., Shi, Y., Beu, S.C., Senko, M.W., Quinn, J.P., Wampler, F.M., McLafferty, F.W.: Coexisting stable conformation of gaseous protein ions. Proc. Natl. Acad. Sci. U. S. A. **90**, 790–793 (1993)
34. Hemling, M.E., Conboy, J.J., Bean, M.F., Mentzer, M., Carr, S.A.: Gas phase hydrogen / deuterium exchange in electrospray ionization mass spectrometry as a practical tool for structure elucidation. J. Am. Soc. Mass Spectrom. **5**, 434–442 (1994)
35. Campbell, S., Rodgers, M.T., Marzluff, E.M., Beauchamp, J.L.: Deuterium exchange reactions as a probe of biomolecule structure. Fundamental studies of gas phase H/D exchange reactions of protonated glycine oligomers with D_2O, CD_3OD, CD_3CO_2D, and ND_3. J. Am. Chem. Soc. **117**, 12840–12854 (1995)
36. Bohme, D.K.: Proton transport in the catalyzed gas-phase isomerization of protonated molecules. Int. J. Mass Spectrom. Ion Processes **115**, 95–110 (1992)
37. Froelicher, S.W., Freiser, B.S., Squires, R.R.: The $C_3H_5^-$ isomers. Experimental and theoretical studies of tautomeric propenyl ions and the cyclopropyl anion in the gas phase. J. Am. Chem. Soc. **108**, 2853–2862 (1986)
38. O'Hair, R.A.J., Gronert, S., DePuy, C.H., Bowie, J.H.: Gas-phase ion chemistry of the acetic acid enolate anion $[CH_2CO_2H]^-$. J. Am. Chem. Soc. **111**, 3105–3106 (1989)
39. Grabowski, J.J., Cheng, X.: Gas-phase formation of the enolate monoanion of acetic acid by proton abstraction. J. Am. Chem. Soc. **111**, 3106–3108 (1989)
40. Kovačević, B., Schorr, P., Qi, Y., Volmer, D.A.: Decay mechanisms of protonated 4-quinolone antibiotics after electrospray ionization and ion activation. J. Am. Soc. Mass Spectrom. **25**, 1974–1986 (2014)
41. Londry, F.A., Hager, J.W.: Mass selective axial ion ejection from a linear quadrupole ion trap. J. Am. Soc. Mass Spectrom. **14**, 1130–1147 (2003)
42. Lide, D.R.: CRC handbook of chemistry and physics, 74th edn. (1993)
43. Hopkins, W.S., Marta, R.A., McMahon, T.B.: Proton-bound 3-cyanophenylalanine trimethylamine clusters: isomer-specific fragmentation pathways and evidence of gas-phase Zwitterions. J. Phys. Chem. A **117**, 10714–10718 (2013)
44. Lecours, M.J., Chow, W.C.T., Hopkins, W.S.: Density functional theory study of $Rh_nS^{0,+/-}$ and $Rh_{n+1}{}^{0,+/-}$ (n = 1–9). J. Phys. Chem. A **118**, 4278–4287 (2014)
45. Wales, D.J., Doye, J.P.K.: Global optimiziation by basin-hopping and the loweset energy structures of Lennard-Jones clusters containing up to 110 atoms. J. Phys. Chem. A **101**, 5111–5116 (1997)
46. Cornell, W.D., Cieplak, P., Bayly, C.I., Gould, I.R., Merz, K.M., Ferguson, D.M., Spellmeyer, D.C., Fox, T., Caldwell, J.W., Kollman, P.A.: A second generation force field for the simulation of proteins, nucleic acids, and organic molecules. J. Am. Chem. Soc. **117**, 5179–5197 (1995)
47. Becke, A.D.: Density-functional thermochemistry. III. The role of exact exchange. J. Chem. Phys. **98**, 5648–5652 (1993)
48. Lee, C.T., Yang, W.T., Parr, R.G.: Development of the Colle-Salvetti correlation energy formula into a functional of the electron density. Phys. Rev. B **37**, 785–789 (1988)
49. Wiberg, K.B., Rablen, P.R.: Comparison of atomic charges derived via different procedures. J. Comput. Chem. **14**, 1504–1518 (1993)
50. Frisch, M.J., Trucks, G.W., Schlegel, H.B., Scuseria, G.E., Robb, M.A., Cheeseman, J.R., Scalmani, G., Barone, V., Mennucci, B., Petersson, G.A., Nakatsuji, H., Caricato, M., Li, X., Hratchian, H.P., Izmaylov, A.F., Bloino, J., Zheng, G., Sonnenberg, J.L., Hada, M., Ehara, M., Toyota, K., Fukuda, R., Hasegawa, J., Ishida, M., Nakajima, T., Honda, Y., Kitao, O., Nakai, H., Vreven, T., Montgomery, J.A. Jr., Peralta, J.E., Ogliaro, F., Bearpark, M., Heyd, J.J., Brothers, E., Kudin, K.N., Staroverov, V.N., Kobayashi, R., Normand, J., Raghavachari, K., Rendell, A., Burant, J.C., Iyengar, S.S.,

Tomasi, J., Cossi, M., Rega, N., Millam, J.M., Klene, M., Knox, J.E., Cross, J.B., Bakken, V., Adamo, C., Jaramillo, J., Gomperts, R., Stratmann, R.E., Yazyev, O., Austin, A. J., Cammi, R., Pomelli, C., Ochterski, J.W., Martin, R.L., Morokuma, K., Zakrzewski, V. G., Voth, G.A., Salvador, P., Dannenberg, J.J., Dapprich, S., Daniels, A.D., Farkas, Ö., Foresman, J.B., Ortiz, J.V., Cioslowski, J., Fox, D.J. Gaussian, Inc.: Wallingford, CT (2009)

51. Elstner, M., Porezag, D., Jungnickel, G., Elsner, J., Haugk, M., Frauenheim, T., Suhai, S., Seifert, G.: Self-consistent-charge density-functional tight-binding method for simulations of complex materials properties. Phys. Rev. B **58**, 7260–7268 (1998)
52. Porezag, D., Frauenheim, T., Kohler, T., Seifert, G., Kaschner, R.: Construction of tight-binding-like potentials on the basis of density-functional theory: application to carbon. Phys. Rev. B **51**, 12947–12957 (1995)
53. Stewart, J.J.P.: Optimization of parameters for semiempirical methods V: modification of NDDO approximations and application to 70 elements. J. Mol. Model. **13**, 1173–1213 (2007)
54. Tian, Z., Kass, S.R.: Gas-phase versus liquid-phase structures by electrospray ionization mass spectrometry. Angew. Chem. Int. Ed. **48**, 1321–1323 (2009)
55. Schmidt, J., Meyer, M.M., Spector, I., Kass, S.R.: Infrared multiphoton dissociation spectroscopy study of protonated p-aminobenzoic acid: does electrospray ionizaton afford the amino- or carboxy-protonated ion? J. Phys. Chem. A **115**, 7625–7632 (2011)
56. Tang, L., Kebarle, P.: Effect of the conductivity of the electrosprayed solution on the electrospray current. Factors determining analyte sensitivity in electrospray mass spectrometry. Anal. Chem. **63**, 2709–2715 (1991)
57. Ikonomou, M.G., Blades, A.T., Kebarle, P.: Electrospray-ion spray: a comparison of mechanisms and performance. Anal. Chem. **63**, 1989–1998 (1991)
58. Zhou, S., Hamburger, M.: Effects of solvent composition on molecular ion response in electrospray mass spectrometry: investigation of the ionization processes. Rapid Commun. Mass Spectrom. **9**, 1516–1521 (1995)
59. Amad, M.H., Cech, N.B., Jackson, G.S., Enke, C.G.: Importance of gas-phase proton affinities in determining the electrospray ionization response for analytes and solvents. J. Mass Spectrom. **35**, 784–789 (2000)
60. Hunt, D.F., Sethi, S.K.: Gas-phase ion-molecule isotope-exchange reactions – methodology for counting hydrogen atoms in specific organic structural environments by chemical ionziation mass spectrometry. J. Am. Chem. Soc. **102**, 6953–6963 (1980)
61. Hunter, E.P.L., Lias, S.G.: National Institute of Standards and Technology: NIST Chemistry WebBook. (2005)
62. de Grotthuss, C.J.T.: Sur la decomposition de l'eau et des corps qu'elle tient en dissolution a l'aide de l'electricite galvanique. Ann. Chim. (Paris) **58**, 54–73 (1806)
63. Kumler, W.D., Strait, L.A.: The ultraviolet absorption spectra and resonance in benzene derivatives—sulfanilamide, metanilamide, p-aminobenzoic acid, benzenesulfonamide, benzoic acid aniline. J. Am. Chem. Soc. **65**, 2349–2354 (1943)
64. Chang, T.M., Prell, J.S., Warrick, E.R., Williams, E.R.: Where's the charge? Protonation sites in gaseous ions change with hydration. J. Am. Chem. Soc. **134**, 15805–15813 (2012)
65. Thomson, B.A.: Declustering and fragmentation of protein ions from an electrospray ion source. J. Am. Soc. Mass Spectrom. **8**, 1053–1058 (1997)